RESEARCH ARTICLE

Macromolecular Chemistry and Physics
www.mcp-journal.de

Hydrophobic *Bombyx mori* Silk Fibroin: Routes to Functionalization with Alkyl Chains

*Giorgio Rizzo, Carola Ricciardelli, Eloisa Sardella, Roberta Musio, Marco Lo Presti, Danilo Vona, Fiorenzo G. Omenetto, and Gianluca Maria Farinola**

***Bombyx mori* silk fibroin (SF) is a very versatile biopolymer due to its biocompatibility and exceptional mechanical properties which make possible its use as a functional material in several applications. SF can be modified with a large variety of chemical approaches which endow the material with tailored chemical–physical properties. Here, a systematic investigation of different routes is reported to graft long alkyl chains on SF based on both liquid- and solid-phase, aiming to modulate its hydrophobic behavior. The liquid phase method involves direct activation of SF tyrosine residues via diazo coupling and cycloaddition reactions, generating hydrophobic materials insoluble in any common solvent. The solid phase approach consists of the chemical modification of drop-casted SF films by esterification of hydroxyl groups of serine, threonine, and tyrosine SF residues with acyl chlorides of fatty acids. For the solid-state functionalization, a new class of hydrophobic pendant groups is synthesized, based on triple esters of gallic acid anhydrides, that are reacted with the biopolymer to further enhance its resulting hydrophobic features.**

1. Introduction

Silk is a complex protein-polymer composite spun into fibers by different animals, characterized by extraordinary mechanical properties, such as high tensile strength and extensibility, as well as biological compatibility.[1] The extraordinary mechanical properties are thought to be dependent on the molecular assembly of silk fibroins.[2,3] Among them, *Bombyx mori* silk fibroin (SF) represents the most easily available and very versatile biomaterial, suitable for various applications such as biomedical tissue engineering and drug delivery.[3–6] Due to its chemical inertness and excellent mechanical resistance, SF has been used as a biological support for catalysis, selectively interacting with specific molecules and metal ions and acting as an efficient carrier with wide applicability in many fields of material sciences.[7–10] SF has been also used for application in optoelectronics and optics, due to its unique ability to interact with light.[11,12] Moreover, SF behaves as a biocompatible bulk material for in vivo applications, and its degradation can be easily tuned through variation of its β-sheet content.[13] One remarkable feature often required in bioderived materials is modulable hydrophobicity, which can be useful, for example, to increase material durability in aqueous biological media. Moreover, surface polarity plays a key role in specific cell adherence and proliferation, and in the adhesive properties of the biopolymer toward polar/apolar surfaces.[14,15] SF has a relatively simple amino acid composition. In fact, it is mainly composed of glycine and alanine whose concentrations are 45.9% and 30.3%, respectively.[16] Then lower percentages of serine (12%), tyrosine (5.3%), threonine (0.9%), glutamic acid (0.6%), and aspartic acid (0.5%) are present. These latter are the reactive SF amino acids prone to be chemically functionalized.[16,17] Carbodiimide coupling with acid residues of glutamic and aspartic acids has been reported, although the resulting biomaterial functionalization was limited due to the low content of these residues.[18,19] SF amino groups of lysines and arginines have been crosslinked with glutaraldehyde to graft large biomacromolecules to the SF backbone.[20] Direct anchorage to free —OH residues or aromatic substitution reactions on SF serine and tyrosine moieties have also been explored.[17] Tyrosine coupling with cyanuric chlorides for the conjugation of PEG chains or polysaccharides has been reported.[21,22] Sulfation reactions of tyrosine are also known, although experimental conditions with chlorosulfonic acid or sulfuric acid severely hydrolyze the polymer backbone, irreversibly modifying the native polymer structure.[23] Other modification

G. Rizzo, C. Ricciardelli, R. Musio, D. Vona, G. M. Farinola
Department of Chemistry
University of Bari Aldo Moro
via Edoardo Orabona 4, Bari 70126, Italy
E-mail: gianlucamaria.farinola@uniba.it
E. Sardella
CNR-Institute of Nanotechnology (CNR-NANOTEC) UoS Bari
c/o Department of Chemistry
University of Bari Aldo Moro
via Edoardo Orabona 4, Bari 70126, Italy
M. L. Presti, F. G. Omenetto
Silklab, Department of Biomedical Engineering
Tufts University
4 Colby Street, Medford, MA 02155, USA

The ORCID identification number(s) for the author(s) of this article can be found under https://doi.org/10.1002/macp.202300145

DOI: 10.1002/macp.202300145

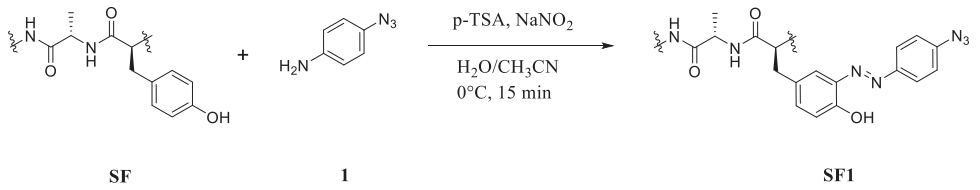

Scheme 1. Synthesis of diazocompounds using 4-azidoanline and silk fibroin tyrosine residues.

routes include enzyme-catalyzed tyrosine reactions and diazonium salt coupling processes on phenolic rings.[24] Recently, fluorinated SF has been developed as a coating for biomedical applications.[25] Since SF is not soluble and rapidly collapses in solvents different from water, the variety of chemical reactions suitable for SF modification is limited. Furthermore, modification processes are requested to be fast and quantitative, involving mild conditions, such as low temperatures, weak bases and acids, and moderately reactive reactants, to prevent irreversible denaturation of the protein backbone.

Here we report two different chemical approaches to modulation of hydrophobicity in SF-derived materials based upon chemical modification of side chain amino acids both in liquid and solid phase.

In the first approach, we investigated the diazo coupling reactions on SF tyrosine residues in the liquid phase, which fulfills the above-mentioned requisites of processes for SF modification. This route is reported as an easily available and mild process for SF treatment in aqueous solutions since it is performed at low temperatures and under slightly basic conditions in which SF is completely stable.[26,27] Moreover, tyrosine is homogeneously distributed throughout the SF backbone, thus allowing an extensive chemical modification with a good degree of order and repeatability.[28,29] The diazotized SF has subsequently been subjected to cycloaddition reactions with terminal alkynes bearing long alkyl chains. A second approach, based on solid-phase chemical modification of drop-casted SF films, is based on the direct esterification of the OH-bearing amino acids (serine, threonine, and tyrosine) with long chain fatty acids acyl chlorides, thus reaching a significantly high degree of functionalization. Finally, highly hydrophobic gallic acid-derived anhydrides have been synthesized and anchored to SF, generating derivatives with a high degree of hydrophobicity due to the high content of long-chain pendants in the final structure.

2. Results and Discussions

2.1. Synthesis of Chemically Modified Silk Fibroin

2.1.1. Liquid Phase Diazotization and Cycloaddition Reactions

A 5% SF aqueous solution (50 mg mL^{-1}) was used as the starting material for chemical functionalization. Diazo coupling on tyrosine residues with *p*-azidoaniline followed by Huisgen Cu(I) catalyzed cycloaddition reaction on azide pendant groups was investigated for the functionalization of SF in aqueous conditions.[27,30] To assess the effect of the stoichiometry ratio correct equivalent ratio between tyrosine residues in the SF and the 4-azidoaniline diazotization partner, a systematic change of their equivalent ratio was investigated.[31,32]

A series of diazotization products were obtained (see Table S1, Supporting Information) using a SF_{tyr}:4-azidoaniline equivalent ratio ranging from 1:0.0125 up to 1:10 (**Scheme 1**).

The reaction products were characterized by UV–vis, ATR-FTIR, and ^{1}H-NMR spectroscopies, as discussed in Section 2.3. Once established that the best reagent ratio for SF tyrosine functionalization was SF_{tyr}:4-azidoaniline 1:1, we used the obtained SF1 polymer in a click-reaction with 1-hexadecyne to allow the formation of the triazole unit with the residual azide SF groups. The synthesis was performed not only in a convergent pathway based on the 1,3-dipolar Cu(I) catalyzed Huisgen cycloaddition on the SF diazoadduct (step-by-step synthesis) but also directly linking the hydrophobic triazole to the SF backbone (one-pot synthesis) (**Scheme 2**).

The one-pot pathway consisted of a diazo coupling of SF with the pre-synthesized diazo triazole derivative T4. Different stoichiometric ratios were used, and the resulting materials were characterized by FTIR analyses (see Section 2.3.1) and contact angle kinetics measurements after thin film deposition (see Section 2.4). Quantitative functionalization of tyrosine was demonstrated for SF:-N_3 ratio of 1:4, and different samples were synthesized, ranging from pure SF to 1:4 material. Experimental synthetic conditions are listed in Table S2, Supporting Information.

Different pendant groups of different lengths (**Scheme 3**) were tested to evaluate their effect on the hydrophobic properties of SF. Namely, the long-chain alkynes C_{12}, C_{14}, and C_{18} were used in the one-pot pathway, using the SF:Triazole 1:1 ratio as the best ratio for functionalization.

2.2. Esterification Reactions of SF Casted Films with Fatty Acid Acyl Chlorides and Anhydrides

To overcome the intrinsic difficulty of solution functionalization protocols (e.g., request of mild conditions, incomplete functionalization), a solid-state approach which consists of directly reacting drop-cast films of the biopolymer with the functionalizing agent has been set up.[33] Starting from the evidence that the most abundant amino acids prone to functionalization are serine, tyrosine, and threonine (for a total of 18.3% in protein weight), all characterized by a free sidechain —OH moiety, we investigated the direct esterification of these groups in the solid state through reaction with fatty acid acyl chlorides or anhydrides. The solvent chosen was anhydrous chloroform since both acyl chlorides and SF films are stable in it. Activation of films toward esterification was performed with an organic base (e.g., triethylamine), used in slight excess with respect to the acylating agent in order to neutralize the HCl produced from the esterification reaction and hence to avoid acid-catalyzed hydrolysis of the SF film. As for the

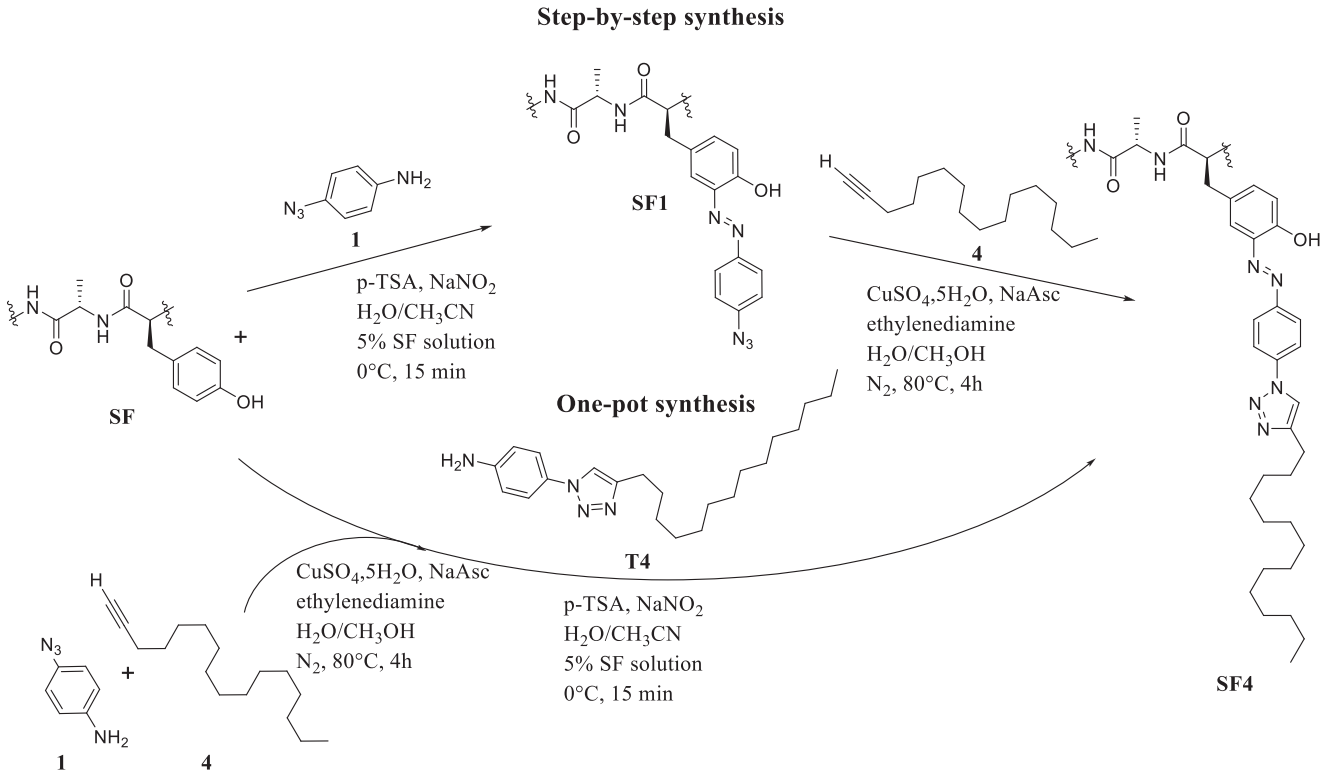

Scheme 2. Schematic convergent synthesis of hydrophobic SF-derived materials. In the upper part is reported the step-by-step synthesis, involving a consequential derivatization of the polymer. In the lower section, the hydrophobic tail was directly conjugated to the SF backbone through a diazo coupling.

SF functionalization in the liquid phase, a standard SF 5% solution was used preliminarily to drop-cast films, using 1 mL of solution which was let air-dry on a Teflon 2.5 × 2.5 cm square dish. Films with 100 nm thickness and 50 mg weight were obtained. We tested different chain-length acyl chlorides, from lauroyl (C12) to stearoyl chloride (C18), increasing by two —CH_2— each fatty acid. The unsaturated fatty acid oleoyl chloride (C18 Δ^9) and linoleoyl chloride (C18 $\Delta^{9,12}$) were used to evaluate the hydrophobic behavior in the presence of unsaturated bonds. Finally, we tested perfluorododecanoyl chloride to assess an effect on perfluoroalkyl chains.

Drop-cast SF films were reacted with acyl chlorides as reported in **Scheme 4**. SF films are resistant to dissolution in dry organic solvents; hence they were immersed in a chloroform solution containing an excess of acyl chloride, under gentle stirring for 24 h.

Functionalization of SF with higher content of hydrophobic chains was possible by a different approach which consists of increasing the number of chains per single anchoring site. For this reason, inspiration from Nature was taken, thus mimicking the naturally occurring hydrophobic systems, consisting of triesters of glycerol units. We used gallic acid as a functional unit with three alkyl chains exploiting the rigid core of the benzene ring and the carboxylic acid group for final esterification with the OH-bearing amino acid residues. In fact, the reaction of gallic acid with acyl chlorides afforded the triester of the corresponding anhydride that, in basic conditions, can react with the hydroxyl groups of SF, forming an ester bond. Hence, we first performed

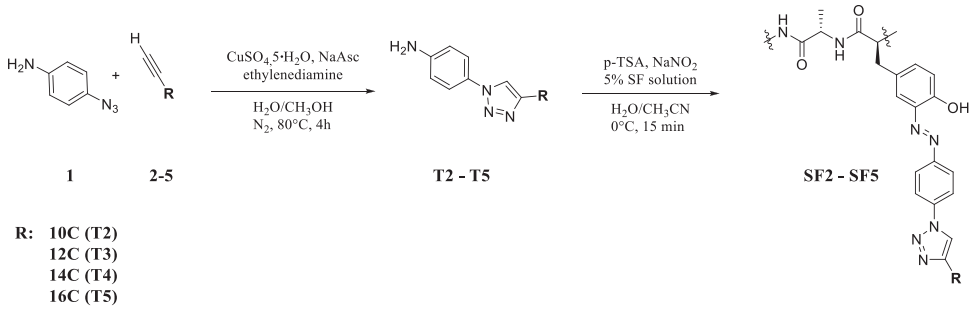

Scheme 3. Synthesis of different hydrophobic triazoles by CuAAC reaction and anchoring to SF through diazonium coupling on tyrosine residues.

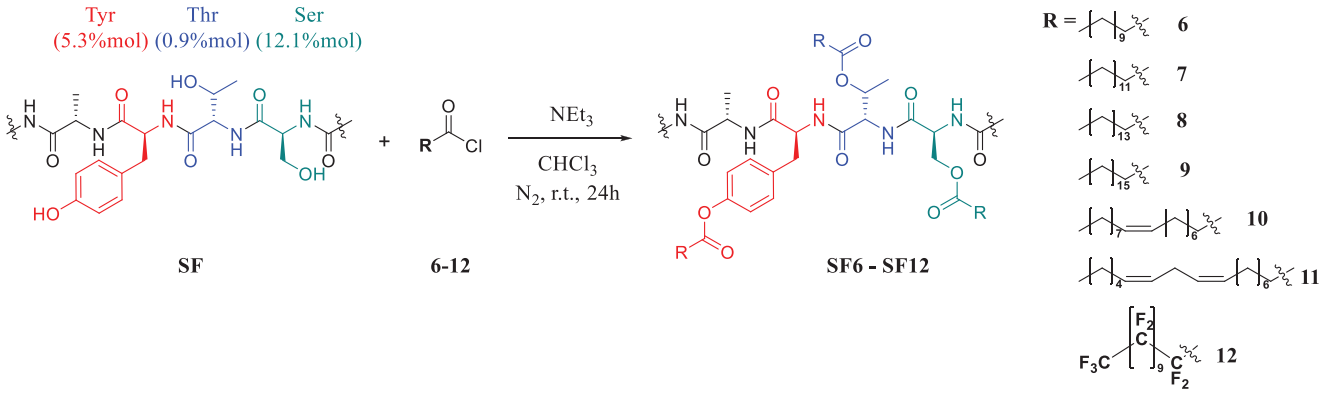

Scheme 4. Anchoring of different acyl chlorides to SF film exploiting the esterification of —OH side chain amino acids. Functional amino acids are highlighted in various colors.

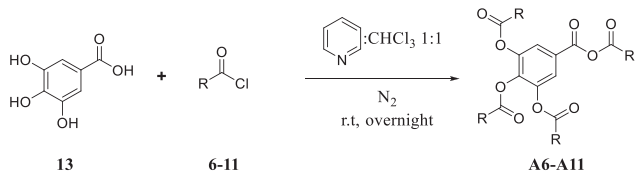

Scheme 5. Synthesis of hydrophobic triple esters of gallic anhydrides.

the reaction of gallic acid with all the above-mentioned acyl chlorides according to **Scheme 5**. Reactions proceeded smoothly, with satisfactory yields for the shortest acyl chlorides, whilst longer chains required a gentle heating to 40 °C to promote homogenization of the reaction media due to the wax-like consistency of some chlorides. The hindrance caused by double bonds in oleic and linoleic derivatives caused a significant drop in yields.

Once synthetized the anhydrides A6-A11, they were reacted with SF cast films using the same protocol reported for the functionalization of SF with acyl chlorides (**Scheme 6**). In principle, this approach triplicates the degree of substitution, since each free —OH aminoacidic residue was functionalized with a pendant bearing three hydrophobic alkyl chains.

A complete characterization of hydrophobic SF-films SF6-SF12 and SFA6-SFA11 was not possible due to the low solubility of the functionalized materials in any common solvent, precluding direct quantification of the degree of functionalization with acyl chlorides or gallic acid anhydrides. Nonetheless, according to previous results obtained with soluble derived polymers using triazoles (SF2-SF5) in which a complete functionalization of tyrosine was achieved with 4 equivalents of hydrophobic pendant, corresponding to 1.43 mmol of triazole for 100 mg of SF, we used a large excess of acyl chlorides or gallic acid anhydrides tackling complete functionalization in solid SF films. More specifically, 13.58 mmol of acyl chloride was used for each derived SF film in a solid-state reaction (SF6-SF12), meaning ten times stoichiometric excess of the reactant with respect to the calculated tyrosine residues. In the case of the gallic acid anhydride, 1.86 mmol was used, corresponding to a 1.3-time excess of the hydrophobic linker (SFA6-SFA11). Considering also that SF films could be functionalized only on the surface of the material and not in the whole protein structure in the dry state, an even higher excess of reactants with respect to SF was likely used.

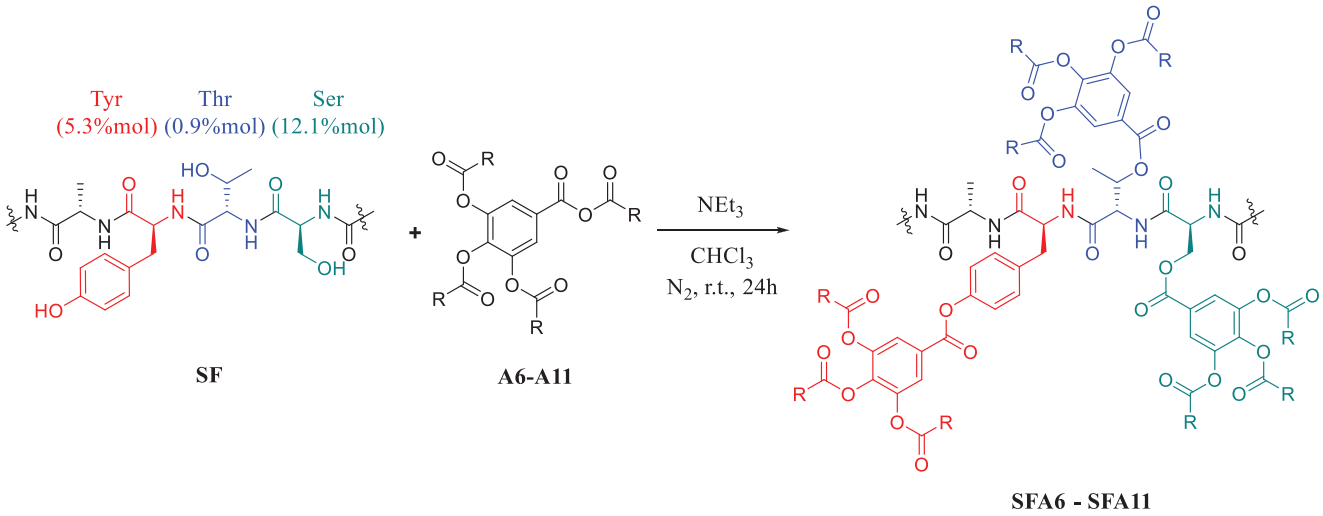

Scheme 6. Anchoring of different anhydrides to SF film exploiting the esterification of —OH side chain amino acids. Functional amino acids are red, blue, and green highlighted.

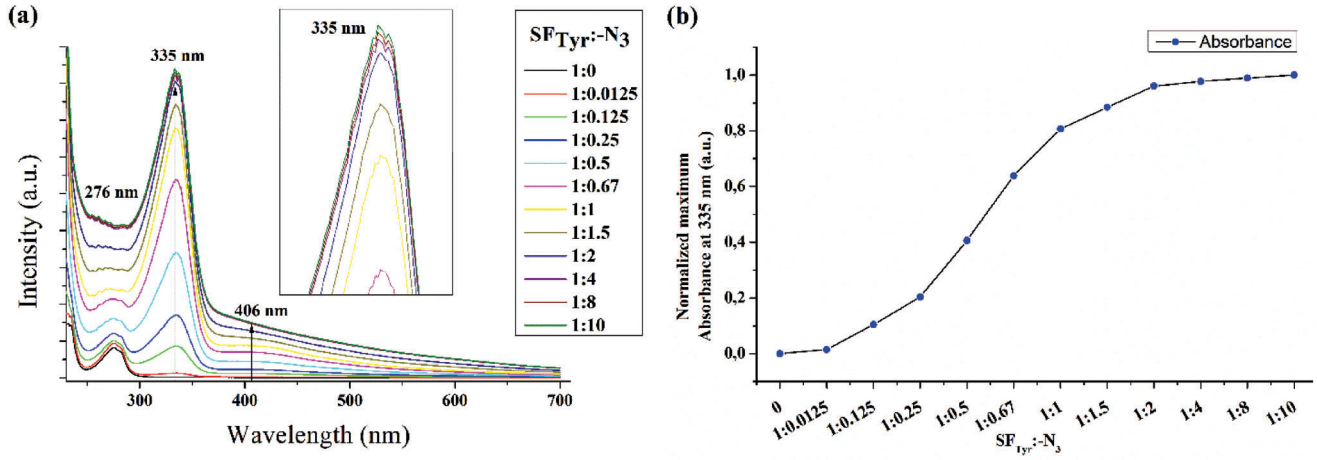

Figure 1. UV–vis spectra of SF1 polymers obtained by diazotization reaction of SF with 4-azidoaniline. a) Superimposed spectra, showing the typical absorption peak of free tyrosines at 276 nm and the absorption peak of diazocompound at 335 and 406 nm. The absorption peak at 335 nm was magnified in the inset to show the superimposable UV–vis spectra of completely diazotized samples. b) Titration curve using the maximum absorbance value at 335 nm for each sample, showing a saturation over the 1:4 SF_{tyr}:N_3 equivalent ratio.

2.3. Characterization of Functionalized SF Polymers

2.3.1. Spectroscopic Characterization of Diazotized SF1

SF1 polymers resulting from the diazotization with *p*-azido aniline reactions were characterized by UV–vis spectroscopy, ATR-FTIR on air-dried films, and ^{1}H-NMR spectroscopy. UV–vis spectra are reported in **Figure 1**.

The first spectrum in black is referred to as pure SF solution, showing only a weak broadened peak near 280 nm, due to π–π^* tyrosine transitions. Subsequent addition of 4-azidoaniline determined an increase in absorbance near 335 nm, referred to typical absorption π–π^* band for diazo compounds. The increase of diazotization grade, starting from 0.5 equivalents of 4-azidoaniline (Figure 1, cyan curve), promotes a broadened band centered at about 400 nm referred to n–π^* transitions in diazo compounds.[34] Diazotization reaction becomes almost quantitative for an equivalent ratio of 1:4 in 4-azidoaniline. In fact, 1:4, 1:8, and 1:10 ratios showed nearly the same absorbance value at 335 nm, suggesting a complete diazotization process of tyrosine residues. Figure 1 also reports all maximum normalized absorbance values at 335 nm, clearly showing a saturation curve for diazo compounds in SF.

All samples were then air-dried and analyzed with ATR-FTIR spectroscopy (**Figure 2**). N—H stretching, N—H bending, and C—N stretching vibrational bands at ≈1650, 1540, and 1230 cm^{-1}, respectively are diagnostic.[35] In 4-azidoaniline-SF adducts, only appreciable N—H bending variations are detected, corresponding to the band at 1513 cm^{-1} in pure SF (black curve, 1:0). For increasing amount of 4-azidoaniline, a systematic shift toward

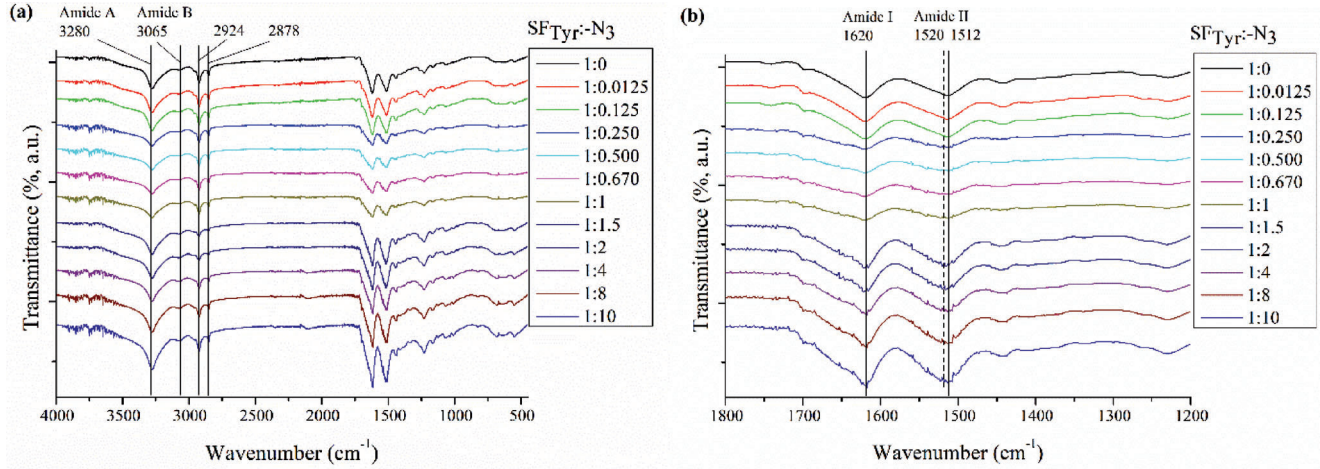

Figure 2. ATR-FTIR of SF1 films obtained by air-drying of diazotized SF solutions. a) Complete ATR-FTIR spectra and b) magnification of Amide I and Amide II bands. Amide bands are bold highlighted. Amide II band showed a significant peak shifting from 1512 cm^{-1} for pure SF film (1:0) to 1520 cm^{-1} in 1:4, 1:8, and 1:10 diazotized SF films. A shift for this absorption band is directly correlated with a decrease in β-sheet content and hence a lower crystallinity in the whole SF matrix.

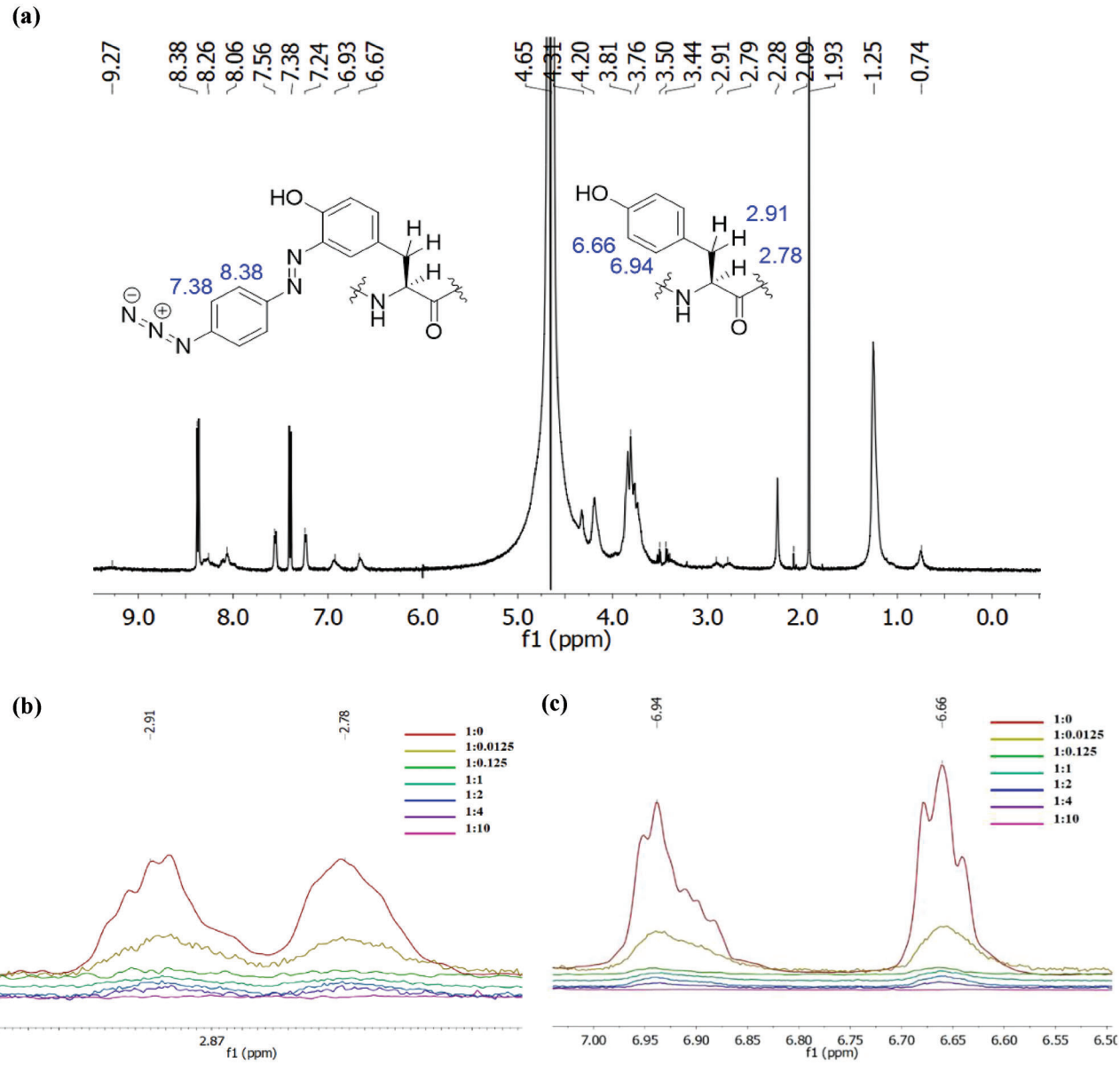

Figure 3. ^{1}H-NMR results for diazotized SF solutions. A typical NMR spectrum is reported in (a), with molecule insets and relative proton labeling. In (b) and (c) all the NMR spectra are superimposed, showing the aromatic and the aliphatic regions, respectively. For both observed signals, almost a quantitative diazo coupling is reached for SF_{tyr}:-N_3 1:4 equivalent ratio.

higher wavenumbers is observed, ranging from 1512 cm^{-1} in SF, up to 1520 cm^{-1} for 1:2, 1:4, 1:8, and 1:10 systems. A signal shift is highlighted with dashed lines in Figure 2b. Since H-bonding in polypeptides is related to the ability to form tight intermolecular and intramolecular interactions, an increase in the signal for N—H bending vibrations could be attributed to a stabilization of the N—H bond, inhibiting other weak interactions such as H-bonding with other peptide strands.[36] This evidence can be directly associated with the partial β-sheet disruption due to the presence of a new aromatic ring in the structure.

Diazotized **SF1** samples were also characterized via ^{1}H-NMR spectroscopy, performing analyses in D_2O after 6 h of dialysis against ultrapure water. Spectra are reported in **Figure 3**.

Tyrosine signals at 2.78, 2.91, 6.66, and 6.94 ppm were monitored during the diazotization reactions. Due to the proximity to the diazo adduct, changes in the chemical shift can be observed. Tyrosine aliphatic signals at 2.79 δ (Hα) and 2.90 δ (Hβ) and aromatic signals at 6.94 δ (Hδ) and 6.66 δ (Hϵ) were studied instead of those of the new diazo adduct since residual unreacted 4-azidoaniline in SF samples can affect the assignment of signals to the final compounds. Unfunctionalized and functionalized SF tyrosine signals can be assigned as reported in the literature.[37–39]

NMR titration confirmed the maximum equivalent ratio between SF_{tyr} and 4-azidoaniline, since the 1:4 ratio (Figure 2, violet curve) gave almost a quantitative diazotization, as it can be seen

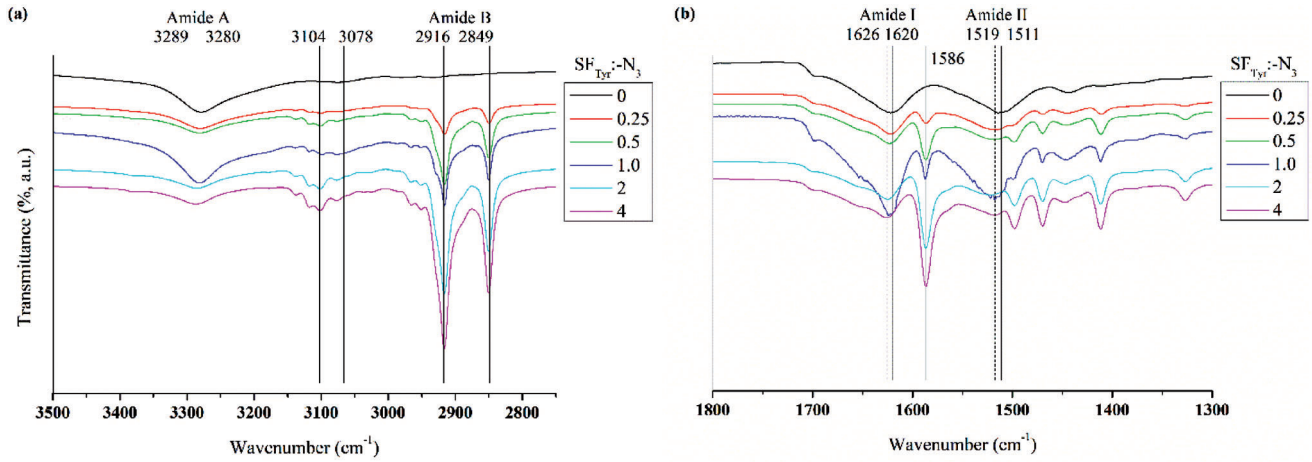

Figure 4. Infrared absorption spectra for the triazole functionalized SF4 from the one-pot approach. a) Absorption band shift for Amide A; b) adsorption bands shift for Amide I and Amide II, respectively.

by NMR spectra whose free tyrosine signals decrease to zero with an increasing amount of aniline.

2.3.2. Spectroscopic Characterization of Triazole Functionalized SF4 Polymers

Scarce solubility of SF4 polymers in any common solvent prevented their characterization via NMR spectroscopy. Therefore, the characterization was performed using ATR-FTIR analyses. Data collected from ATR-FTIR spectra of triazole functionalized **SF4** are shown in Figure S1, Supporting Information, and confirm that both step-by-step and one-pot methods are suitable to covalently link the hydrophobic alkynyl moiety to the SF backbone. In fact, both samples exhibit intense absorption bands in the range 2750–3000 cm^{-1} due to the presence of the long aliphatic chains. Moreover, the fingerprint region confirms the presence of triazole linkers.[40] In fact, the triazole linker can be recognized by the formation of new vibrational bands: 1588 and 1471 cm^{-1} peaks are referred to as C═C and C—N stretching vibrations, respectively.[41] Also, a new intense peak at 3095 cm^{-1} that partially overlaps with the SF band B, confirms the C—H stretching in the 5-position of the triazole.[42] The step-by-step method results in a less controlled cyclization process, since some unreacted —N$_3$ pendant groups are still present, as confirmed by asymmetric stretching vibrations at ≈2286 cm^{-1}. Conversely, the one-pot method leads to a quantitative addition to the SF backbone, without leaving free unreacted groups. Probably, the lower degree of functionalization in the step-by-step approach may be due to the gradual increase of hydrophobicity as the Huisgen reaction proceeds, which makes some of the diazo groups eventually less accessible.

Comparison of ATR-FTIR spectra of **SF4** samples synthesized by the more efficient one-pot method revealed a significant vibrational shift of the typical SF bands Amide A (3279 cm^{-1}), Amide I (1621 cm^{-1}), and Amide II (1512 cm^{-1}), as it can be seen in the FTIR insets in **Figure 4**. Amide A band linearly shifted to 3287 cm^{-1} in sample 6 whose hydrophobic tail reached the maximum concentration. A decrease in wavenumbers in the Amide I and Amide II bands is directly referred to as a decrease in the crystallinity of the materials since these bands are associated with the β-sheet variations. In fact, Amide I increased from 1621 to 1626 cm^{-1}, whilst Amide II shifted from 1512 to 1519 cm^{-1}. The crystallinity decrease can be attributed to the presence of long hydrophobic chains that interfere with the β-sheet variations since an even more intense variation is observed for a higher functionalization degree in SF. Quantitative FTIR shifts are listed in **Table 1**.

2.4. Wettability Investigation by Water Contact Angle Analysis

The measurement of wettability in water of **SF4** samples was tested by means of the sessile drop method. As reported in **Figure 5**, a decrease in the droplet volume was registered for the sample used as the control (Entry 1, Table 1) within the first 2 s of acquisition time. On the other hand, regardless of the chemical modification performed on SF, a total absence of water absorption was observed, with the exception of entry 5 (Table 1) where a slight water absorption occurs.

Although ATR-FTIR spectra highlight an increase of polymer crystallinity upon progressive chemical modification with hydrophobic triazole pendants, contact angle measurements showed a poor variation of water contact angle (WCA) in terms of the total amount of hydrophobic pendant groups anchored.

Table 1. Observed infrared absorption spectra for Amide A, Amide I, and Amide II bands for the hydrophobic SF derivatives.

Entry	SF$_{Tyr}$/triazole ratio	Amide A [cm^{-1}]	Amide I [cm^{-1}]	Amide II [cm^{-1}]
1	1:0	3279	1621	1512
2	1:0.25	3280	1623	1516
3	1:0.5	3280	1623	1517
4	1:1	3282	1623	1518
5	1:2	3284	1625	1521
6	1:4	3287	1626	1519

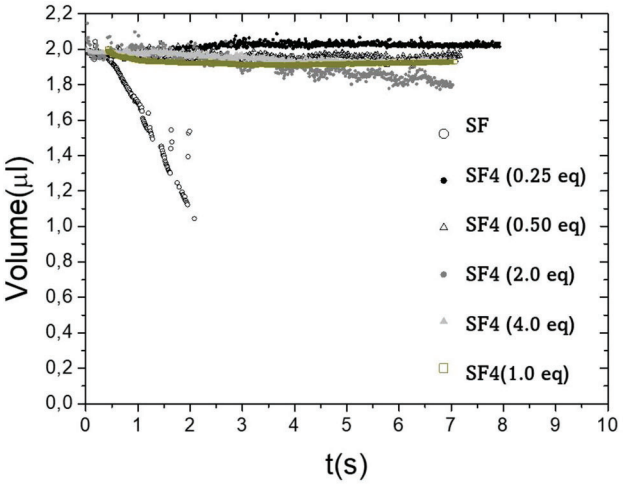

Figure 5. Droplet volume as a function of the acquisition time (s). White dots refer to unmodified SF, whereas its hydrophilicity is reflected in the dramatic decrease of droplet volume within the first acquisition frames.

In fact, all the samples exhibit an average WCA of 80°, with best performances for SF polymers functionalized over SF:Triazole 1:1 ratio, as shown by the lower standard deviations for these samples.

A complete collection of all the WCA values is reported in **Table 2**.

Besides the increasing lengths of the pendant chains bound to **SF4** products in Scheme 3, the corresponding WCA values did not change significantly. Only a slight increase in hydrophobic angles was observed increasing the chain lengths. The lowest WCA was found for the shortest chains obtained from 1-dodecyne **SF2** and 1-tetradecyne **SF3** (60 ± 8 and 70 ± 10, respectively), whilst the triazole obtained from 1-octadecyne **SF5** showed the highest WCA, reaching a mean value of 80° (Table 2), with a maximum value of 92° (80 ± 12).

With regard to SF cast film functionalized with fatty acyl chlorides (**SF6-SF12**), WCAs showed that the samples improved water resistance since they are completely stable under droplet contact. Moreover, films recovered as optically transparent and flexible materials, are progressively more hydrophobic with the length increase of acyl chloride. Starting with the shortest chains, an increase of WCA from 81 ± 6 for **SF6** to 84 ± 12 for **SF9** was observed. The presence of a double bond, as for oleoyl chloride in **SF10**, decreased the WCA down to 60°. Further insaturations, such as linoleoyl chloride in **SF11**, decreased the value to 50°, making the film more hydrophilic. Finally, as expected, the presence of perfluoroalkyl chains dramatically improved the hydrophobic behavior of SF film to 100° in **SF12**. The non-perfluorinated C12 chain from lauroyl chloride **SF6** showed a WCA of 81°.

Table 2. All WCA (°) reported for the three classes of chemically modified SF derivatives.

Compound	Functionalization [R]	WCA [°]
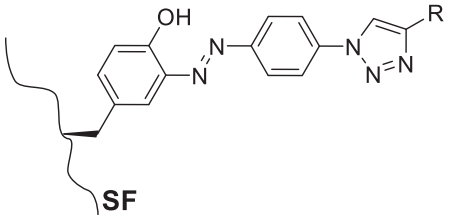	SF2 (10 C)	60 ± 8
	SF3 (12 C)	70 ± 10
	SF4 (14 C)	82 ± 7
	SF5 (16 C)	80 ± 12
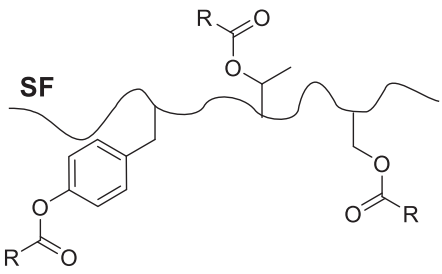	SF6 (11 C)	81 ± 6
	SF7 (13 C)	100 ± 16
	SF8 (15 C)	97 ± 10
	SF9 (17 C)	84 ± 12
	SF10 (17 C *cis*-Δ9)	60 ± 10
	SF11 (17 C *cis*,*cis*- Δ9,12)	50 ± 15
	SF12 (11 C perfluoro-)	100 ± 13
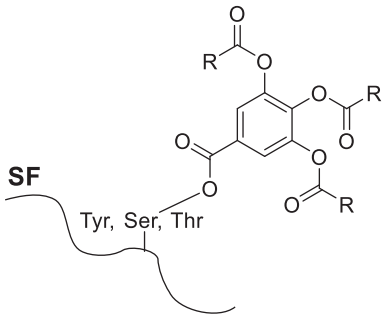	SFA6 (11 C)	105 ± 12
	SFA7 (13 C)	109 ± 5
	SFA8 (15 C)	97 ± 26
	SFA9 (17 C)	109 ± 13
	SFA10 (17 C *cis*-Δ9)	60 ± 15
	SFA11 (17 C *cis*,*cis*- Δ9,12)	52 ± 10

Regarding the SF functionalized with gallic acid triester moieties reported in Table 2 (**SFA6-SFA11**), WCAs increased to high values, with a minimum of 105° for the shortest chain **SFA6**, to a maximum of 122° for the triester of the longest tail **SFA9**, thus paving the way to highly hydrophobic SF-based materials. Also in this case, as well as for functionalization with acyl chlorides, the presence of double bonds in **SFA10** and **SFA11** caused a dramatic decrease of WCA down to 60 ± 15 and 52 ± 10 for oleoyl and linoleoyl chains, respectively.

3. Conclusions

Different functionalization routes have been explored to graft long alkyl chains on the SF backbone aiming to increase its hydrophobicity. Aliphatic chains of different lengths, the presence of unsaturated bonds, and a perfluoroalkyl moiety have been explored. A systematic approach is reported to establish the degree of functionalization in the liquid phase via diazotization coupling on tyrosine residues, further reacting the terminal azide unit with long-chain alkynes in the copper-catalyzed azido-alkyne cycloaddition, a versatile and quantitative click chemistry reaction. Upon different lengths, the hydrophobic behavior of bioderived SF materials did not change significantly, showing an improved water resistance independently on the anchored pendant.

A higher degree of functionalization was achieved with heterogeneous chemistry on drop-casted SF films in chloroform solutions. In this case, ad hoc hydrophobic pendants were synthetized mimicking the natural hydrophobic materials based on triesters of glycerol. In fact, gallic acid was chosen as a glycerol-like moiety bearing three hydroxyl groups and a carboxylic group for further anchoring to free hydroxyl groups of SF films. Also in this case, different lengths of pendants and various degrees of unsaturation were tested, showing the best results with the longest chains. In both liquid and solid phase SF chemical modification approaches, the presence of *cis*-double bonds decreases the hydrophobic behavior, whereas the presence of fluorine atoms highly increases the WCAs of the samples.

Our investigation reports a versatile chemistry that can be in principle extended to various kinds of chemical groups useful to endow silk fibroin with tunable chemical behavior.

4. Experimental Section

General Procedure: All reagents and solvents were used without any further purification steps. Raw *B. mori* silk cocoons were purchased from Tajima Shoji, Japan. ATR-FTIR spectra were acquired with a Perkin Elmer UATR Two spectrophotometer, using a 2 × 2 mm diamond, acquiring spectra in the spectral window 400–4000 cm^{-1}, using a 1 cm^{-1} resolution, a 1 cm^{-1} acquisition interval, and 8 scans for each sample. For the ATR-FTIR analyses, the following abbreviations were used: sh = sharp; b = broadened; vb = very broadened; s = strong; m = medium; w = weak. ^{1}H-NMR and ^{13}C-NMR spectra were acquired with an Agilent500-vnmrs500 spectrometer at 25 °C, using 500 and 125 MHz for the ^{1}H-NMR and ^{13}C-NMR analyses, respectively. Spectra were acquired a 11.7 Tesla, with a typical spectral width of 9000 Hz for ^{1}H and 31250 Hz for ^{13}C, using a 90° observing pulse. UV–vis measurements were recorded with UV–vis Cary 5000 double-ray spectrophotometer (Agilent Technologies – USA), ranging from 250 to 700 nm, using a 1 nm resolution. Solutions were properly diluted for a concentration of ≈100 μg mL^{-1}. UV–vis spectra were normalized relatively to the sample concentrations. The hydrophilic character of pristine and modified materials was measured by means of dynamic WCA that was carried out at room temperature by a CAM200 digital goniometer (KSV instruments), equipped with a Basler A602 high-speed camera. Three measures per sample were performed by a sessile drop technique. A drop (2 μL) of double distilled water was placed on the sample and a fast mode acquisition (speed camera settings: 512 × 485 pixels,130 fps) was used to study the absorption phenomena on plasma-treated surfaces. The interaction of the liquid with the surface was monitored with a CCD camera and the contact angle was evaluated both by fitting the drop profile with a Young/Laplace model and by using the tangent calculation method. In the case of samples that adsorb water WCA(t) values and volume of the drop, V(t) were plotted versus time of acquisition and fitted with linear fit. The rate of adsorption, Δv(μL)/Δt(s), was evaluated by calculating the angular coefficient of the straight line. Finally, the WCA_{t0} was considered as a measure of the wettability of the material especially for materials on which WCA values changed quickly due to absorption or super-hydrophilic character. All the derivatives of hydrophobic SF were characterized by ATR-FTIR analyses and WCA since they were not soluble in any common solvent.

Degumming SF: Degummed SF was obtained from *B. mori* cocoons according to the procedures described previously.[43] 5g of cocoons were shredded and boiled for 30 min in a 2 L 0.02 M Na_2CO_3 solution, then rinsed several times with bidistilled water to remove the residual sericins and the excess salt. The mat was fully dried at room temperature for 24 h.

Preparation of SF Aqueous Solution: The dried degummed SF (2 g) was dissolved in 8 mL 10.4 M LiBr aqueous solution at 60 °C for 4 h. The fibroin-LiBr solution was dialyzed against bidistilled water using a regenerated cellulose dialysis membrane (MWCO 12.400 g mol^{-1}) to remove LiBr. Dialysis water was changed after 20 min, 2 h, 6 h, and finally every 24 h for 4 days. The last dialysis step was performed in saline borate buffer (0.15 M NaCl and 0.1 M $Na_2B_4O_7$ at pH 9). The dialyzed SF solution was centrifugated at 10 000 rpm for 1 h at 4 °C, then filtered with a 100 μm Millipore filter and stored at 4 °C. The final concentration of the SF aqueous solution was 8.8 wt% (88 mg mL^{-1}). With an appropriate volume of buffer solution, the SF sample was diluted to 5 wt% (50 mg mL^{-1}).

Preparation of SF Films: SF thin flexible and optically transparent films were obtained with a drop-casting method, using 1 mL of 5 wt% solution of SF dropped on a flat Teflon dish with a standard 2.5 × 2.5 cm surface. Solutions were slowly evaporated at room temperature for 24 h. Dried films weighed 50 mg and profilometry analyses gave a typical film thickness of about 100 nm.

Supporting Information

Supporting Information is available from the Wiley Online Library or from the author.

Acknowledgements

Roberto Gristina and Antonio Palermo are gratefully acknowledged for their technical support in statistical analyses and NMR analyses, respectively.

Conflict of Interest

The authors declare no conflict of interest.

Data Availability Statement

The data that support the findings of this study are available in the supplementary material of this article.

Keywords

Bombyx mori silk fibroin, diazo coupling, functionalization of tyrosine, liquid phase chemical modification, solid phase chemical modification

Received: May 15, 2023
Revised: August 4, 2023
Published online: September 22, 2023

[1] T. Asakura, K. Isobe, A. Aoki, S. Kametani, *Macromolecules* **2015**, *48*, 8062.
[2] J. M. Gosline, P. A. Guerette, C. S. Ortlepp, K. N. Savage, *J. Exp. Biol.* **1999**, *202*, 3295.
[3] B. B. Mandal, S. C. Kundu, *Biotechnol. Bioeng.* **2008**, *100*, 1237.
[4] M. Mondal, K. Trivedy, K. S. Nirmal, *Caspian J. Env. Sci.* **2007**, *5*, 63.
[5] O. Hakimi, D. P. Knight, F. Vollrath, P. Vadgama, *Composites, Part B* **2007**, *38*, 324.
[6] C. Vepari, D. L. Kaplan, *Prog. Polym. Sci.* **2007**, *32*, 991.
[7] G. Rizzo, G. Albano, M. L. Presti, A. Milella, F. G. Omenetto, G. M. Farinola, *Eur. J. Org. Chem.* **2020**, *2020*, 6992.
[8] G. Rizzo, G. Albano, T. Sibillano, C. Giannini, R. Musio, F. G. Omenetto, G. M. Farinola, *Eur. J. Org. Chem.* **2022**, *2022*, e202101567.
[9] G. Rizzo, M. L. Presti, C. Giannini, T. Sibillano, A. Milella, G. Matzeu, R. Musio, F. G. Omenetto, G. M. Farinola, *Macromol. Chem. Phys.* **2020**, *221*, 2000066.
[10] G. Rizzo, M. L. Presti, C. Giannini, T. Sibillano, A. Milella, G. Guidetti, R. Musio, F. G. Omenetto, G. M. Farinola, *Front. Bioeng. Biotechnol.* **2021**, *9*, 653033.
[11] F. G. Omenetto, D. L. Kaplan, *Nat. Photonics* **2008**, *2*, 641.
[12] D.-H. Kim, N. Lu, R. Ma, Y.-S. Kim, R.-H. Kim, S. Wang, J. Wu, S. M. Won, H. Tao, A. Islam, *Science* **2011**, *333*, 838.
[13] B. D. Lawrence, M. Cronin-Golomb, I. Georgakoudi, D. L. Kaplan, F. G. Omenetto, *Biomacromolecules* **2008**, *9*, 1214.
[14] M. S. Kim, Y. N. Shin, M. H. Cho, S. H. Kim, S. K. Kim, Y. H. Cho, G. Khang, I. W. Lee, H. B. Lee, *Tissue Eng.* **2007**, *13*, 2095.
[15] M. L. Presti, G. Rizzo, G. M. Farinola, F. G. Omenetto, *J. Adv. Sci.* **2021**, *8*, 2170100.
[16] A. R. Murphy, D. L. Kaplan, *J. Mater. Chem.* **2009**, *19*, 6443.
[17] C. Z. Zhou, F. Confalonieri, M. Jacquet, R. Perasso, Z. G. Li, J. Janin, *Proteins* **2001**, *44*, 119.
[18] S. Sofia, M. B. McCarthy, G. Gronowicz, D. L. Kaplan, *J. Biomed. Mater. Res.* **2001**, *54*, 139.
[19] C. P. Vepari, D. L. Kaplan, *Biotechnol. Bioeng.* **2006**, *93*, 1130.
[20] Y. Q. Zhang, Y. Ma, Y. Y. Xia, W. D. Shen, J. P. Mao, X. M. Zha, K. Shirai, K. Kiguchi, *J. Biomed. Mater. Res., Part B* **2006**, *79B*, 275.
[21] Y. Gotoh, S. Niimi, T. Hayakawa, T. Miyashita, *Biomaterials* **2004**, *25*, 1131.
[22] T. Kardestuncer, M. B. McCarthy, V. Karageorgiou, D. Kaplan, G. Gronowicz, *Clin. Orthop. Relat. Res.* **2006**, *448*, 234.
[23] Y. Tamada, *Biomaterials* **2004**, *25*, 377.
[24] G. Freddi, A. Anghileri, S. Sampaio, J. Buchert, P. Monti, P. Taddei, *J. Biotechnol.* **2006**, *125*, 281.
[25] J. N. Fountain, M. J. Hawker, L. Hartle, J. Wu, V. Montanari, J. K. Sahoo, L. M. Davis, D. L. Kaplan, K. Kumar, *ChemBioChem* **2022**, *23*, 202200429.
[26] A. R. Murphy, P. S. John, D. L. Kaplan, *Biomaterials* **2008**, *29*, 2829.
[27] H. Zhao, E. Heusler, G. Jones, L. Li, V. Werner, O. Germershaus, J. Ritzer, T. Luehmann, L. Meinel, *J. Struct. Biol.* **2014**, *186*, 420.
[28] Y. Takahashi, M. Gehoh, K. Yuzuriha, *Int. J. Biol. Macromol.* **1999**, *24*, 127.
[29] C.-Z. Zhou, F. Confalonieri, N. Medina, Y. Zivanovic, C. Esnault, T. Yang, M. Jacquet, J. Janin, M. Duguet, R. Perasso, *Nucleic Acids Res.* **2000**, *28*, 2413.
[30] S. Bräse, C. Gil, K. Knepper, V. Zimmermann, *Angew. Chem., Int. Ed.* **2005**, *44*, 5188.
[31] J. Andersen, U. Madsen, F. Bjoerkling, X. Liang, *Synlett* **2005**, *2005*, 2209.
[32] K. D. Grimes, A. Gupte, C. C. Aldrich, *Synth* **2010**, *2010*, 1441.
[33] L. Raynal, B. J. Allardyce, X. Wang, R. J. Dilley, R. Rajkhowa, L. C. Henderson, *J. Mater. Chem. B* **2018**, *6*, 8037.
[34] G. J. Pielak, M. S. Urdea, K. Igi, J. I. Legg, *Biochemistry* **1984**, *23*, 589.
[35] X. Hu, D. Kaplan, P. Cebe, *Macromolecules* **2006**, *39*, 6161.
[36] J. Zhao, J. Wang, *J. Phys. Chem. B* **2015**, *119*, 14831.
[37] T. T. Le, Y. Park, T. V. Chirila, P. J. Halley, A. K. Whittaker, *Biomaterials* **2008**, *29*, 4268.
[38] C. J. Sims, D. T. Fujito, D. R. Burholt, J. Dadok, H. R. Giles, D. A. Wilkinson, *Prenatal Diagn.* **1993**, *13*, 473.
[39] M. Nagura, H. Ishikawa, *Polym. J.* **1979**, *11*, 159.
[40] V. Y. Grinshtein, A. A. Strazdin, A. K. Grinvalde, *Chem* **1970**, *6*, 231.
[41] S. Cao, Z. Pei, Y. Xu, R. Zhang, Y. Pei, *RSC Adv.* **2015**, *5*, 45888.
[42] K. Zamani, K. Faghihi, M. Sangi, J. Zolgharnein, *Turk. J. Chem.* **2003**, *27*, 119.
[43] D. N. Rockwood, R. C. Preda, T. Yücel, X. Wang, M. L. Lovett, D. L. Kaplan, *Nat. Protoc.* **2011**, *6*, 1612.

